46th Annual Review of Progress in Quantitative Nondestructive Evaluation
QNDE2019
July 14-19, 2019, Portland, OR, USA

QNDE2019-6866

EFFICIENT INCORPORATION OF VISCO-ELASTIC BEHAVIORS AND THIN INTERMEDIATE LAYERS IN TRANSIENT FINITE ELEMENT MODELING OF LAMINATE STRUCTURES

Alexandre Imperiale[1], Nicolas Leymarie, Edouard Demaldent
CEA LIST
Gyf-sur-Yvette, France

ABSTRACT

Anisotropic laminated materials such as composite structures is an important class of materials intensively used in high-end industrial contexts. Analyzing ultrasonic testing experiments of these materials through numerical modeling remains an important task, especially in the presence of complex phenomena such as visco-elastic behavior and structural noise emanating from intermediate epoxy layers. This communication is dedicated to recent advances aiming at representing these phenomena into a finite element solver in transient regime. Concerning the visco-elasticity we consider the standard models of Kelvin-Voigt, Maxwell and Zener. After recapping their corresponding attenuation behaviors, we propose an efficient calibration strategy for these models, valid for 2D and 3D anisotropic solids. We analyze relevant time discretization strategies for each model, leading to an efficient explicit numerical scheme. Concerning the structural noise, we propose to incorporate the effect of epoxy layers using spring-mass transmission conditions between plies. These transmission conditions are adequately embedded in the finite element formulation using the mortar element method. Illustrations of our combined numerical tools are given in a 2D context.

Keywords: laminate composite structures, ultrasonic testing, visco-elasticity, structural noise, transient finite elements

1. INTRODUCTION

Modeling ultrasonic testing experiments of laminate composites requires simulating the propagation of elastic bulk waves in a medium with varying anisotropic directions, i.e. per stratum and following the potential curvature of the specimen. We focus our attention to numerical approaches in order to represent accurately complex geometrical features (stiffeners, cracks, specimen curvatures …). Additionally, in the context of laminate composite structures, at least two important aspects should be addressed: (1) attenuation of the ultrasonic beam due to both resin viscosity and multiple diffractions at the fiber scale; (2) thin intermediate epoxy layers (from 5 to 15 μm) inducing a structural noise around specific cutting frequencies.

In previous communications [1] we have detailed a numerical approach in time domain and based upon a decomposition of the configuration into macro-elements (MEs). In this approach, each ME bears capital information concerning both the geometry and the physical characteristics (fluid, solid, stratified, absorbing layers …) of a sub-domain. The MEs are sub-discretized in a structured fashion depending on an *a priori* estimation of the wavelengths of interest and a high-order explicit numerical scheme is applied leading to significantly enhanced performances of the overall numerical solver. The different physical formulations assigned to each macro-element are linked together using the mortar element method [2], which conserves, in the case of conform interface meshes, the explicit nature of the numerical scheme. This strategy has been successfully used in the context of immersed curved composite laminates in a 3D context.

In this communication, we detail improvements of the finite element solver, which are twofold. First, we propose to calibrate and incorporate standard visco-elasticity models [3] in order to take into account attenuation phenomena and we replace thin intermediate epoxy layers by effective transmission conditions based upon a spring-mass rheological model [4]. The related explicit numerical scheme are presented along with their corresponding stability condition on the time step (so-called CFL condition) and practical considerations on the performances of the numerical solver are discussed. We propose illustrations on a simple case of a 2D laminate composite specimen.

2. MODELLING ATTENUATION PHENOMENA

2.1 Anisotropic visco-elasticity

Let us denote by u the particle displacement field emanating from the ultrasonic perturbation, and satisfying the field equation

[1] Contact author: alexandre.imperiale@cea.fr

$\rho\partial_{tt}^2 u = \nabla\cdot\sigma$, where ρ is the mass density of the solid and σ is the stress tensor. In the inviscid case, the constitutive law simply reads $\sigma = \mathcal{C}\varepsilon$, where ε is the strain tensor and $\mathcal{C}$ is the fourth-order symmetric and positive elasticity tensor. This standard modeling setup naturally leads to a conservative dynamical system, which limits its application, especially in the case of laminate composite structures where attenuation phenomena cannot be neglected. To account for these phenomena we resort to the class of visco-elastic models in which the constitutive law is expressed as the convolution between a relaxation function ψ and the strain rate

$$\sigma = \psi * \partial_t\varepsilon = \partial_t\psi * \varepsilon.$$

Traditionally, see e.g. [3], a visco-elastic law is characterized through its complex modulus $\mathcal{F}(\partial_t\psi)(\omega) = \mathcal{C}(\omega) + \imath\mathcal{D}(\omega)$, where the ratio $\mathcal{Q}(\omega) = \mathcal{D}(\omega)^{-1}\mathcal{C}(\omega)$ is the so-called quality factor. From a practical standpoint, experiments aiming at characterizing the material at hand may lead to measured phase velocity and attenuation factors for different incident angles and various frequencies. From these measures it is possible [5] to identify relevant real and imaginary parts of the complex modulus with a description of their dependences w.r.t. the frequency. In the perspective of transient numerical modelling, we often resort to using standard visco-elastic models having local-in-time (without convolution) expression of their constitutive laws. These models entail specific dependences of the corresponding attenuation laws and, in any case, need to be calibrate in order to fit with the identified mechanical parameters.

2.2 Calibration of standard visco-elastic models

We consider in the following three standard visco-elastic models [3]: the model of Kelvin-Voigt (KV) defined by $\sigma = \mathcal{C}^{KV}\,\varepsilon + \mathcal{D}^{KV}\,\partial_t\varepsilon$, the model of Maxwell (MX) where $(\mathcal{D}^{MX})^{-1}\sigma + (\mathcal{C}^{MX})^{-1}\partial_t\sigma = \partial_t\varepsilon$, and the model of Zener (ZN) with $\sigma + \tau^{ZN}\partial_t\sigma = \mathcal{C}^{ZN}\,\varepsilon + \tau^{ZN}\mathcal{D}^{ZN}\,\partial_t\varepsilon$, where τ^{ZN} is a scalar value corresponding to a relaxation time. We propose a calibration strategy aiming at satisfying the real part $\mathcal{C}_*$ and imaginary part $\mathcal{D}_*$ of a target identified complex modulus at a specific target angular frequency ω_*. This calibration strategy, based upon a so-called "low loss" assumption is simple enough to be applied in a 2D and 3D setting, with generally anisotropic target complex modulus. Furthermore, it corresponds to practical NDT configurations where the mechanical parameters of the specimen at hand are often known on a restricted frequency bandwidth. The choice of a specific visco-elastic model is performed according to their corresponding attenuation law which are quadratic, constant or locally linear (w.r.t. to the frequency) for the KV, MX and ZN models respectively.

2.3 Explicit time discretization

In order to keep the performances of the numerical solver available in the inviscid case, we consider explicit time discretization for the three models, thus avoiding the resolution of a linear system at each iteration. This class of discretization procedure leads to stable algorithm upon a so-called CFL condition on the time-step. In our work, we follow the energy arguments [6] in order to present the CFL condition for the standard visco-elastic models. In particular, we can express the specific difficulties underlying the KV model, which requires a decentered treatment of the viscous term in order to remain explicit. This particular aspect gives a more restrictive stability condition compared to the MX and ZN time schemes, whose CFL conditions are only slightly modified by the introduction of the viscosity.

2.4 Illustration on a 2D visco-elastic laminate

As an illustration, we consider a simple 2D configuration of 20 orthotropic plies of 250µm thickness staggered together to form a 10mm thick specimen. The fiber orientation in each ply vary from 0° to 90°, the latter corresponding to an out-of-plane fiber direction. The various target parameters, considered at a target frequency $f_* = 6$ MHz, are given in Table 1.

Angle	C_{*11} (GPa)	C_{*12}	C_{*22}	C_{*33}
0°	143.2	7.5	15.8	7.0
90°	15.8	8.2	15.8	3.8

Angle	D_{*11} (GPa)	D_{*12}	D_{*22}	D_{*33}
0°	15.1	0.75	1.5	0.56
90°	1.5	0.75	1.5	0.56

TABLE 1: TARGET MECHANICAL PROPERTIES. MASS DENSITY AT $\rho = 1.6\ g\cdot cm^{-3}$.

We show in Figure 1 the snapshot of the solution obtained in the inviscid case compared to the snapshots obtained with the KV, MX and ZN models. The very good agreement between these snapshots illustrate the validity of our calibration approach. A closer look at the solution obtained in the viscous cases shows slight changes in the wave fronts due to the different nature of the attenuation law of each visco-elastic model.

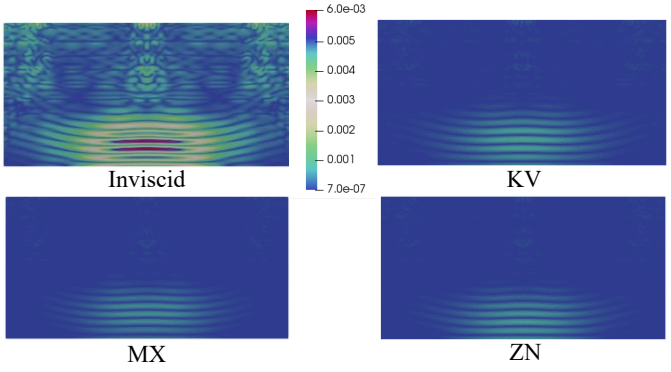

FIGURE 1: COMPARING THE MAGNITUDE OF THE DISPLACEMENT FIELD AFTER 2µs.

In Table 2 we compare the number of time-steps required for each model to reach the same final simulation time. Choosing the inviscid case as a reference, we observe the effect of the significantly more restrictive stability condition of the KV model compared to MX and ZN.

	Inviscid	KV	MX	ZN
Δt (µs)	$19 \cdot 10^{-4}$	$7 \cdot 10^{-4}$	$19 \cdot 10^{-4}$	$18 \cdot 10^{-4}$
# steps	1024	2841	1029	1073

TABLE 2: COMPARING TIME-STEPS FOR 2µs TIME WINDOW.

3. MODELING THIN INTERMEDIATE LAYERS

A specific characteristic of ultrasonic testing of laminates is their potential cutting bandwidth due to the resonance of the plies interfaces media. This phenomenon is modeled by considering thin (typically from 5µm to 15µm) intermediate layers usually of epoxy material [7]. Dedicated numerical strategy, such as "anisotropic order" of approximation [1], may be employed in this context. However, it often entails significant deformations of mesh elements, penalizing in term the CFL stability condition.

To alleviate completely the difficulty we propose to model these thin epoxy layers using a spring-mass model [4]. In essence, this model consists in perturbing the displacement field and normal stress continuity relations at the interface by incorporating compliance terms and inertial terms respectively. In our approach, the spring-mass model between each neighboring plies are incorporated within the numerical solver using the mortar element method [2]. By doing so, we can prove that for every model considered, namely Inviscid, KV, MX and ZN, the CFL stability condition is not modified by the compliance and inertial parameters of the "imperfect" interface.

To illustrate this aspect of our modeling strategy, we consider a configuration of 20 plies of 242.5µm, separated by 19 epoxy layers of 7.5µm. The epoxy layers are assumed to be inviscid isotropic materials, with a density of ρ = 1.6 $g \cdot cm^{-3}$ and Lamé coefficients of $\lambda = 4.4$ GPa and $\mu = 1.6$ GPa.

In Figure 2 we compare two numerical approaches in the purely elastic case. In the first one, as proposed in [1], each intermediate layers are meshed bearing a reduced order discretization in the thickness direction. In the second one, we use our new strategy using a spring-mass model within the mortar element approach. We observe a very good agreement between the two numerical solutions, and most importantly, the ability of the "imperfect" interfaces strategy to render accurately the structural noise appearing in this configuration.

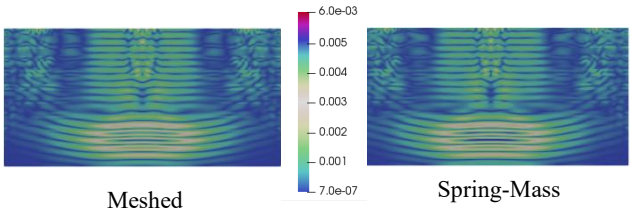

FIGURE 2: MESHED VS. SPRING-MASS MODEL FOR REPRESENTING INTERMEDIATE EPOXY LAYERS.

In Table 3, we obtain a significant gain in the number of time-steps required to reach the same simulation time. This gain grows larger as the thickness of the epoxy layers decreases.

	Meshed	Spring-Mass
Δt (µs)	$6 \cdot 10^{-4}$	$12 \cdot 10^{-4}$
# steps	3316	1598

TABLE 3: COMPARING TIME-STEPS FOR MESHED VS. SPRING MASS MODEL.

Finally, we can illustrate the combined effect of visco-elasticity for the KV, MX and ZN cases with intermediate epoxy layers incorporated using a spring-mass model.

4. CONCLUSION AND PERSPECTIVES

In our work we propose a calibration strategy for standard visco-elasticity models and we analyze their corresponding explicit time-discretization in a finite element procedure. We also consider spring-mass models to represent thin intermediate epoxy layers between plies and we use the flexibility of the mortar element method to incorporate this approach adequately, without perturbing the stability of the time-discretization. It should be noted that the presented work naturally extends to 3D configurations. Ongoing work and perspectives are the use of inhomogeneous spring mass model to represent complex delamination flaws or the application of visco-elastic models in other UT configuration such as weld inspection simulation.

REFERENCES

[1] Imperiale, A., and Demaldent, E., 2019, "A Macro-Element Strategy Based upon Spectral Finite Elements and Mortar Elements for Transient Wave Propagation Modeling. Application to Ultrasonic Testing of Laminate Composite Materials," accepted for publication in Int. J. Numer. Methods. Eng.

[2] Hauret, P., and Le Tallec, P., 2007, "A Discontinuous Stabilized Mortar Method for General 3D Elastic Problems," Comput. Methods in Appl. Mech. Eng., **196**(49), pp. 4881–4900.

[3] Carcione, J. M., 2014, *Wave Fields in Real Media, Volume 38: Wave Propagation in Anisotropic, Anelastic, Porous and Electromagnetic Media*, Elsevier Science, Amsterdam.

[4] Lombard, B., and Piraux, J., 2003, "How to Incorporate the Spring-Mass Conditions in Finite-Difference Schemes," SIAM J. Sci. Comput., **24**(4), pp. 1379–1407.

[5] Deschamps, M., and Hosten, B., 1992, "The Effects of Viscoelasticity on the Reflection and Transmission of Ultrasonic Waves by an Orthotropic Plate," The Journal of the Acoustical Society of America, **91**(4), pp. 2007–2015.

[6] Bécache, E., Ezziani, A., and Joly, P., 2005, "A Mixed Finite Element Approach for Viscoelastic Wave Propagation," Comput Geosci, **8**(3), pp. 255–299.

[7] Wang, L., and Rokhlin, S. I., 2003, "Ultrasonic Wave Interaction with Multidirectional Composites: Modeling and Experiment," The Journal of the Acoustical Society of America, **114**(5), pp. 2582–2595.